X-622-68-39
PREPRINT

NASA TM X-63197

A TROPICAL CYCLONE DEVELOPMENT AS REVEALED BY NIMBUS II HIGH RESOLUTION INFRARED AND ESSA-3 TELEVISION DATA

GUENTER WARNECKE
LEWIS J. ALLISON
EARL R. KREINS
LARRY M. McMILLIN

JANUARY 1968

GSFC

GODDARD SPACE FLIGHT CENTER
GREENBELT, MARYLAND

A TROPICAL CYCLONE DEVELOPMENT AS REVEALED BY NIMBUS II HIGH RESOLUTION INFRARED AND ESSA-3 TELEVISION DATA

By

Guenter Warnecke
Goddard Space Flight Center*
Greenbelt, Maryland, USA

Lewis J. Allison
Goddard Space Flight Center
Greenbelt, Maryland, USA

Earl R. Kreins, Major, USAF
USAF Environmental Technical Applications Center
Washington, D.C., USA

Larry M. McMillin
Allied Research Associates, Inc.
Concord, Massachusetts, USA

Paper Presented at Fifth Technical Conference on Hurricanes and Tropical Meteorology, 21 November 1967, Caracas, Venezuela.

*On leave from the Free University of Berlin, Germany as National Academy of Sciences-National Research Council Senior Postdoctoral Resident Research Associate with the National Aeronautics and Space Administration.

**Air Weather Service Member temporarily attached to Goddard Space Flight Center.

ABSTRACT

Nimbus II High Resolution Infrared Radiometer (HRIR) data, in combination with ESSA-3 photographs and the sparse conventional observations available from the central Pacific Ocean, were analyzed to determine the early stages of tropical storm development for the case of typhoon "Marie 1966." The meteorological conditions in the area were found to satisfy the requirements commonly considered necessary for tropical storm development in that the sea surface temperature was above 28°C, a deep lower tropospheric moist layer existed, the surface flow was convergent, and the vertical wind shear was small. The mid-Pacific troughs present in both hemispheres and outlined by distinct cloud bands reached with their extremities into the development area. They were also associated with a pronounced upper tropospheric (200 mb) divergence which could mainly be inferred from the cirrus flow visible in the satellite observations and which persisted for a number of days over the region of storm development. This upper divergence seemed to play a major role in the initial development of the storm.

The results of this study prove the usefulness of high resolution infrared and television observations from satellites for the investigation of relatively small scale phenomena in tropical meteorology.

CONTENTS

TABLES

PRECEDING PAGE BLANK NOT FILMED.

A TROPICAL CYCLONE DEVELOPMENT AS REVEALED BY NIMBUS II HIGH RESOLUTION INFRARED AND ESSA-3 TELEVISION DATA

INTRODUCTION

In a comprehensive survey on problems in tropical meteorology, Alaka (1964) wrote the following statement on the broadscale conditions of hurricane and typhoon development:

"It is a known fact that the incidence of hurricanes is directly related to atmospheric conditions beyond the immediate locality of the potential storm. Some of the known pertinent broadscale features include the condition of the trades, the equatorward extension of the middle latitude westerlies and the intensity and location of the subtropical highs and intertropical shearlines. The mechanism of the persistence and variations of these features and the nature and dynamics of their relation to hurricane formation and development need to be investigated."

This paper has two purposes; namely to demonstrate that satellite infrared and television observations can help in the investigation of these mechanisms, and to present the results of a case study performed particularly for the early development stages of typhoon "Marie 1966" by using high resolution observations of the Nimbus II and ESSA-3 meteorological satellites.

While a satellite television picture resembles a normal photograph and needs no explanation, introductory remarks are necessary for the interpretation of high resolution infrared radiometer (HRIR) data used and presented in this report.

HIGH RESOLUTION INFRARED RADIOMETER DATA

The high resolution infrared radiometer (HRIR) of the Nimbus II meteorological satellite measured radiation in the 3.5 - 4.2 micron atmospheric "window" region. Detailed observations of three-dimensional cloud structures were made possible by the relatively small field of view which was 8 x 8 kilometers at the subsatellite point determined by the average satellite altitude of 1100 kilometers and the 0.5 degree aperture of the instrument.

The radiometer measurements differ from satellite television pictures in that the infrared radiometer measures outgoing emitted radiation while the television pictures depict differences in reflected solar radiation. In the 3.5 - 4.2 micron near-infrared region, only nighttime measurements detect pure thermal radiation. Atmospheric and terrestrial features are detected by daytime measurements also, but a separation of the two radiation components, and therefore a unique physical interpretation of the measurements in meteorological terms, is not possible because of the approximately equal radiances of the emitted thermal radiation and the near infrared reflected-solar radiation. In the absence of sunlight, blackbody radiation can be assumed and the detected radiance can be converted to the temperature of the radiating surface ("equivalent blackbody temperature," T_{BB}). This permits one to derive earth or ocean surface temperatures, under clear sky conditions, and cloud top heights when an opaque, plane cloud surface fills the field of view of the radiometer. Examples of this technique and results from satellite experiments are well documented (for example NASA, 1966).

It should be mentioned that in the 3.5 - 4.2 micron range of the HRIR instrument, some slight atmospheric attenuation by water vapor and carbon dioxide is still present and corrections of up to +5°K may have to be applied to the temperature maps. These corrections are proportional to the scan nadir angle and the variable atmospheric water vapor content.

The infrared data are presently available in two forms. One is a photographic image formed scan by scan from the original analog record of the data. This results in a pictorial view of the cloud and surface temperature structure. However, no absolute values of either temperatures or temperature differences can be derived from this display, because reproductions from the original negatives are exposure controlled. In addition, large distortions at the sides of the orbital strips prevent a good mosaic of consecutive orbits. Nevertheless, the photo imagery has the advantage of being the more complete form of data display. An approximate geographic grid which is accurate to within ±2 degrees of great circle arc at the subsatellite point is superimposed upon the photographic image for a rough orientation. Figure 1 is an example of an orbital film strip exhibiting the fully developed typhoon "Marie," the main subject of this study. The vortex center is marked by a cirrus canopy and no 'eye' is discernable. The pronounced convective inflow spiral bands can be distinguished from the thinner and more diffuse cirrus outflow streamers. A large number of structural details can be seen in this photo display, but the obvious distortions at the sides of the filmstrip obscure part of the storm.

The second form of data, the grid print map, is a transformation of the data calibrated in terms of "equivalent blackbody temperature," into a standard geographical map projection (Mercator or polar stereographic) of various scales by means of a large computer. The advantages of this form of presentation are the display of absolute values, the elimination of distortion, and the possibility of automatically composing measurements from consecutive orbits into quasi-synoptic areal maps. However, due to the scanning geometry, either a loss of detail will result from averaging in the center portions of each swath or data gaps will occur at some distance from the subsatellite point where the data spacing is larger than the grid interval. Figure 2 is an example of a computer product showing the rectified composite of numerical data from three consecutive orbits including the one of Figure 1 in a Mercator projection. Automatic contouring helps one to recognize the patterns such as a large spiraling typhoon cloud system (center), the cloud band of the intertropical convergence zone (center right), and extra-tropical frontal cloud systems (upper left and lower right). The average minimum cloud top temperatures in the frontal cloud systems are around 230°K (approximately -40°C and corresponding to an average cloud top height of at least 11 kilometers). The lowest temperature shown over typhoon "Marie" in this map are below 225°K indicating cloud top heights above 11.8 kilometers. Values colder than 230°K should, however, be viewed with some reservation because they are at the lower limits of detection of this radiometer.

The grid print maps used in this study were changed into isopleth pictures and colored for better illustration. The areas shown in blue, dark blue, and purple depict colder areas within a region with a temperature less than 230°K, but no specific temperature values can be assigned to the isopleths delineated by these colors. This is due to the mentioned characteristics of this radiometer.

When interpreting the measured equivalent blackbody temperature as cloud top temperature, an approximate conversion of these values into cloud top height can be performed by use of the 1962 U.S. Standard Atmosphere temperature-height relationship. This relationship was used in the legends of Figures 5, 6, 7, 9, 10, and 11.

DEVELOPMENT OF TYPHOON "MARIE" AS DERIVED FROM SATELLITE OBSERVATIONS

The development of typhoon "Marie" took place in an area between 10°N and 20°N and between 170°W and 170°E during the last week of October 1966. The first indication of significant cloud development connected with the storm was found in this area on 25 October 1966.

Figure 3 is a montage of four HRIR filmstrips obtained from consecutive nighttime orbits on 25 October 1966. The most interesting feature in this figure is the boomerang-shaped cloud system composed of one northern and one southern hemispheric frontal cloud band which join near the equator at 140°E. The intertropical convergence (ITC) zone is indicated by the associated line of convective cloud systems between 5°N and 10°N. The significant feature in the area

of later storm development is a cluster of relatively small convective cloud systems. The different grey shades of these clouds on the original film strip indicate that the cloud tops viewed vary in altitude. Considering the apparent lack of cirrus anvils, and the low radiation temperatures of some of them indicating a high cloud top, it is likely that a number of these clouds have developed into cumulonimbus calvus. The whole cluster appears to be unorganized because the smaller and lower clouds are too small to be resolved by the HRIR instrument.

However, the corresponding ESSA-3 photographs taken 12 hours earlier (Figure 4) show, due to the higher spatial resolution of the camera, that a spiral formation existed within the same cloud cluster; but the photograph does not give any indication of the cloud top heights. Obviously both techniques are useful and when used together provide a means for the early detection of a convergent streamfield, at least at the lower tropospheric cloud level, and the build-up of stronger convective cells within this area.

The analysis of a grid print map, as reproduced in Figure 5, shows the HRIR measurements in a rectified version (Mercator map projection) for the night of 25 October. The boomerang-shaped cloud system and the ITC cloud band stand out clearly. However, no structural details of the cloud cluster mentioned before are resolved because of the averaging of more than 200 measurements into one grid point of the grid print map. In the figure the cluster appears as a small isolated area of lower equivalent blackbody temperature marked by the letter "M."

On the following day, 26 October, the area in question is located at the boundary between two orbits from both the Nimbus II and ESSA-3 satellites and is so distorted on the photographic displays, not shown here, that it is difficult to derive detailed characteristics of the particular cloud cluster. However, an intensification of a number of small convective cloud cells, some of which seem to have developed cirrus anvils, can at least be derived from the television picture, and the Nimbus II grid print map (Figure 6) confirms this by showing an expansion and intensification of the cold spot, marked by "M."

A drastic change occurred during the next 24 hours. On 27 October the HRIR grid print map (Figure 7) shows an extended high (cold) cloud system which seems to merge into the ITC zone of cloudiness between 8°N and 16°N and 170°E and 180° longitude. A detailed photograph of the HRIR data (Figure 8) reveals extended areas of high clouds, a pronounced spiral structure of these high reaching cloud systems, and a strong anticyclonic cirrus outflow. This outflow is suggested by the texture at the outer edges of the high-level spiral clouds. It should be emphasized that the main cirrus outflow occurs over and along the pronounced convective spiral cloud bands while the center of the forming cyclone apparently shows large areas of clear sky. On the next two days, 28 and 29 October, a growing cirrus canopy forms over the center of the developing storm system which in the grid print maps (Figures 9 and 10) now appears as a large high-level (cold) cloud area centered at 15°N, 169°E. The typhoon stage of this storm was reached on 30 October when located near 160°E. The numerical analysis of the

infrared data of 1 November 1966 (Figure 11) shows a large cirrus canopy above 11 kilometers while the HRIR photograph shows the details of the inflow and outflow spirals (Figure 1). A striking feature in this case is the large scale outflow system at the cirrus level which finally penetrates even into the southern hemisphere. This outflow can be assumed as being located at the 200 mb level because, according to Johnson (1966), the cirrus flow seen in satellite pictures was repeatedly found to represent the horizontal motion field at this level.

METEOROLOGICAL ASPECTS OF TYPHOON "MARIE" DEVELOPMENT

The earliest indication of the development of typhoon "Marie" was found, as mentioned before, in the satellite observations of 25 October 1966 close to 15°N latitude and 180° longitude, an area with no weather station closer than 1200 kilometers. Thus the physical state of the troposphere in this region can be obtained only by interpolation of conventional data and inference from the satellite observations.

The development of "Marie" as seen in the satellite data described in the previous section and more extensively treated by Fett (1968) and Warnecke et al. (1968) seems to follow the lines of tropical storm development as recently surveyed by Gray (1967), with the exception of his stated opinion on the negligible importance of upper tropospheric (say 200 mb) divergence for the initial tropical storm development.

Gray's list of necessary conditions for tropical storm development is fulfilled in this case. The distance of the development area from the ITC cloud

band located at 7°N to 8°N in the satellite observations (Figures 3 and 4) was found to be 7° to 8°. This ITC cloud band was assumed to coincide with Gray's equatorial surface pressure trough which could not be located accurately with the sparse conventional data available. The development occurred over water warmer than 26.5°C, since ocean surface temperatures of at least 28°C were detected by the HRIR sensor. This is consistent with the climatological mean temperature for October (Figure 12). The vertical zonal wind shear was very weak in this region, as shown in Table 1. Table 2 which lists radiosonde measurements at the nearest stations shows that this situation was persistent for several days. A deep layer of high relative humidity existed in the lower troposphere, as according to Table 2 the top of the moist layer is in the vicinity of the 700 and 800 mb levels or 2000 m to 3000 m, respectively. Thus the reservoir of latent heat is fairly large. For example, the tropospheric total precipitable water content computed from the radiosonde data over Wake Island on 24 October 1966 was 4.0 cm.

Table 1

Wind on 24 October 1966, 1200 GMT at 15°N, 180°W

(By Horizontal Interpolation from Surrounding Observations)

200 MB	360°, 05 mps
500 MB	080°, 08 mps
700 MB	090°, 10 mps
Surface	080°, 08 mps

Table 2

Radiosonde Measurements in the Vicinity of the Typhoon "Marie" Early Development Area

	October 22, 1966; 00 GMT											
	Johnston Is.				Wake Is.				Majuro Is.			
	Temp	R.H.	Wind		Temp	R.H.	Wind		Temp	R.H.	Wind	
			Deg	mps			Deg	mps			Deg	mps
200 MB	-53	—	182	10	-53	—	130	03	-53	—	216	09
300 MB	-33	53	219	15	-32	18	050	03	-30	20	099	07
400 MB	-17	33	233	10	-18	18	059	16	-15	27	104	06
500 MB	- 6	60	244	06	- 5	17	082	10	- 6	53	089	06
700 MB	9	78	098	03	10	70	104	07	11	33	109	11
800 MB	15	76	083	05	15	71	093	08	16	30	108	09
850 MB	18	63	065	07	17	78	093	11	18	41	105	10
900 MB	21	61	060	08	19	85	087	13	21	59	100	10
950 MB	23	75	056	11	22	80	079	13	23	74	092	08
1000 MB	25	88	074	11	26	83	050	11	29	69	085	06
SFC MB	25	91	080	10	28	87	040	10	30	73	080	05

	October 23, 1966; 00 GMT											
	Johnston Is.				Wake Is.				Majuro Is.			
	Temp	R.H.	Wind		Temp	R.H.	Wind		Temp	R.H.	Wind	
			Deg	mps			Deg	mps			Deg	mps
200 MB	-53	—	276	10	-53	—	005	04	-53	—	300	11
300 MB	-32	24	260	17	-32	16	161	04	-30	19	115	06
400 MB	-16	25	259	14	-17	16	106	12	-15	36	080	08
500 MB	- 6	33	260	06	- 6	15	090	13	- 5	16	106	12
700 MB	11	39	029	04	10	56	091	08	11	32	094	09
800 MB	17	53	044	07	16	61	107	07	15	69	088	08
850 MB	19	63	300	03	18	67	110	07	18	62	100	08
900 MB	21	72	056	08	20	74	114	08	20	66	103	09
950 MB	23	71	060	09	23	72	094	08	23	69	117	05
1000 MB	28	75	058	07	27	75	074	08	28	68	122	04
SFC MB	29	78	060	07	29	82	060	06	30	71	120	03

	October 24, 1966; 00 GMT											
	Johnston Is.				Wake Is.				Majuro Is.			
	Temp	R.H.	Wind		Temp	R.H.	Wind		Temp	R.H.	Wind	
			Deg	mps			Deg	mps			Deg	mps
200 MB	-52	—	264	13	-53	—	355	08	-52	—	290	05
300 MB	-31	14	255	15	-32	18	326	02	-30	27	115	05
400 MB	-17	19	236	05	-16	17	147	02	-15	31	124	04
500 MB	- 8	45	062	07	- 5	17	139	10	- 4	19	128	05
700 MB	9	57	077	16	11	19	104	09	10	49	084	14
800 MB	14	65	076	12	16	67	097	08	15	67	067	08
850 MB	18	68	075	14	18	76	088	11	18	74	078	08
900 MB	21	66	078	12	21	65	089	11	21	73	091	07
950 MB	22	72	082	12	24	84	084	11	24	82	078	05
1000 MB	25	79	086	10	27	84	062	10	28	75	069	05
SFC MB	27	80	090	08	28	84	050	09	29	75	070	05

The large-scale synoptic situation is characterized by the approach of the remnants of a southern and a northern hemispheric extratropical frontal system into the equatorial region. Those frontal remnants can be identified only by their cloud bands as seen in the satellite television pictures and infrared photo imageries as well as upper tropospheric (200 mb level) troughs rather than by conventional surface observations. On 24 October 1966, the day before any obvious indication of the later storm development was present, the cloud photographs show a widely unorganized cumulus convection pattern around 15°N and 180°W. This cumulus convection was activated by the intrusion into this area of the slowly southward moving remnants of a former cold front which is still recognizable in the television and infrared cloud pictures and is associated with a 200 mb streamline trough (Figure 13). In front of this trough a streamline divergence can be observed which persists for a number of days and under which the storm formation takes place. It is this dynamic feature which convinced the authors that high-level divergence is an important factor for the initial tropical storm development and which is contrary to Gray's (1967) statement.

The streamline patterns were from 200 mb wind observations and wind directions derived from the cirrus blown off in distinct bands from the high reaching convective cells, as seen in the satellite observations. This cirrus, in indicating flow direction, actually shows diffluence rather than divergence. A correlation between true horizontal divergence and cirrus cloud patterns has not been established yet for a number of obvious difficulties (Johnson 1966). However, from

the cloud development seen in the satellite pictures in this case, it seems very unlikely that the velocity distribution in the rapidly expanding cirrus bands would compensate the observed diffluence to the extent that no net horizontal divergence would result. Pronounced streamline divergence which, in this sense, strongly suggests wind divergence was found to persist for days over the development area, not only during the later stages of the typhoon but also during the very early stages of detectable development. The 200 mb streamline analyses in addition suggest a coupling between the storm development and the mid-Pacific trough, as described by Sadler (1963 and 1967), since the tropical storm development occurred near the extreme southwestern tip of this trough. The mid-Pacific trough originally introduced as a climatological upper tropospheric feature (Dean 1956) should, however, be interpreted as the result of sequences of extra-tropical fronts penetrating the subtropics and finally stalling in this particular area. This means that the divergence pattern in the streamfield undergoes a continuous cycle of appearance and decay, and the maximum of the resulting divergence will depend on the respective strength and structure of each individual frontal system. A corresponding region where extra-tropical frontal disturbances penetrate the subtropics and stagnate is found in the South Pacific in the same longitudinal area, as seen in TIROS VII radiation data (Allison et al. 1968).

In this particular case, it seems that the anticyclonic flow (Figure 13) north of the almost zonally oriented mid-pacific trough is particularly strong due to the next approaching mid-latitude frontal system. This results in stronger dynamic

effects in the trough region. The high-level diffluence south of the trough seems also to be intensified, at least partly, by two southern hemispheric troughs approaching the same region in phase with the northern hemispheric systems and thus forming the boomerang-shaped large scale cloud configuration mentioned before.

That this configuration of cloud bands, which represent the remnants of former mid-latitude frontal systems, should be considered as an essential factor in the typhoon "Marie" development is also supported by a very similar case of typhoon development, "Gilda" and "Annie" (1967), one year later (Warnecke et al. 1968).

CONCLUSIONS

One of the most significant advantages of remote sensing techniques from a quasi-polar orbiting satellite is the ability to produce global maps of the observed quantities. Thus a wealth of meteorological information is obtained from data sparse areas such as large oceanic areas of the eastern and central Pacific Ocean. In this study, the meteorological conditions over the mid-Pacific Ocean were investigated for part of the typhoon season of 1966. Twelve-hour continuity was provided by the Nimbus II satellite nightly HRIR observations and the ESSA-3 satellite daily television pictures. This information was used in combination with the sparse conventional meteorological data to derive upper and lower tropospheric streamfields and to study the interaction of extra-tropical disturbances

of both hemispheres with the inter-tropical circulation before and during the development of typhoon "Marie 1966."

The development of this typhoon could be followed from the earliest stage of an organized circulation pattern in low-level cumulus around 15°N and 180° longitude through the growth of the convection cloud into cumulonimbus, through the development of cirrus anvils and a cirrus canopy, to the final full typhoon stage. The development was found to take place over the tropical Pacific over a water surface warmer than 28°C, in an area of high water vapor content in the lower troposphere and surface convergence, of weak vertical wind shear, and located 7° to 8° latitude north of the equatorial trough. The development also took place close to an area where the remnants of extra-tropical frontal disturbances, characterized by 200 mb troughs and distinct cloud bands, approached the ITC zone from both hemispheres. Upper tropospheric (200 mb) streamline maps constructed from radiosonde observations as well as satellite pictures (cirrus flow) indicated persistent upper divergence over the development area in connection with these troughs. These seemed to play an essential role in the storm development.

With the presented description of the development history of typhoon "Marie," and particularly the emphasis on the influence of the former mid-latitude frontal disturbances on the divergence pattern over the development area, the authors do not intend to state this kind of development as being the only and main cause of tropical storm development. They want only to say that in the investigated case the described mechanisms seem to have worked. This interaction between

the extra-tropical and tropical circulations certainly is only one of several ways a tropical storm may develop, since stronger upper-tropospheric divergence, intensifying the pre-existing surface convergence and the consequently continuous and widespread convective heat release, may occur under a number of configurations of meteorological systems other than the one discussed here. More cases have to be studied in order to cover the full spectrum of possible conditions. Satellite infrared and television data from near-earth orbits are, as was found, already very useful diagnostic tools for tropical meteorological research. Future use of similar observations, also from geo-synchronous orbits, should provide an even better insight into tropical circulation phenomena.

REFERENCES

Alaka, M. A., 1964: Problems of tropical meteorology (a survey). Technical Note No. 62, World Meteorological Organization, Geneva, Switzerland.

Allison, L. J., E. R. Kreins, F. A. Godshall, and G. Warnecke, 1968: Monthly global circulation characteristics as reflected in TIROS VII radiometric measurements. NASA Technical Note, Goddard Space Flight Center, Greenbelt, Maryland. (In preparation)

Dean, G. A., 1956: The 1955 mean monthly wind circulation over the tropical central Pacific area. Paper No. 2, Contract No. AF 19 (604) - 546, Institute of Geophysics, University of California, Los Angeles, California.

Fett, R. W., 1968: Typhoon formation within the zone of the ITC. Monthly Weather Review, 96(2), 106-117.

Gray, W. M., 1967: Global view of the origin of tropical disturbances and storms. Atmospheric Science Paper No. 114, Department of Atmospheric Science, Colorado State University, Fort Collins, Colorado.

Johnson, H. M., 1966: Motions in the upper troposphere as revealed by satellite-observed cirrus formations. ESSA Technical Report NESC-39, Environmental Science Services Administration, National Environmental Satellite Center, Washington, D.C.

National Aeronautics and Space Administration, 1966: Observations from the Nimbus I meteorological satellite. NASA Special Publication-89, National Aeronautics and Space Administration, Washington, D.C.

Sadler, J.M., 1963: Utilization of meteorological satellite cloud data in tropical meteorology. Proceedings of the First International Symposium on Rocket and Satellite Meteorology, North-Holland Publishing Company, Amsterdam, The Netherlands, 333-356.

Sadler, J.M., 1967: The tropical upper tropospheric trough as a secondary source of typhoons and a primary source of tradewind disturbances. Final Report HIG-67-12, Contract No. AF19 (628)-3860, Hawaii Institute of Geophysics, University of Hawaii, Honolulu, Hawaii.

U.S. Naval Oceanographic Office, 1968: Sea surface isotherms. U.S. Naval Oceanographic Office, Physical Property Section, Washington, D.C. (Unpublished data).

Warnecke, G., L. J. Allison, E. R. Kreins, and L. M. McMillin, 1968: The development of Typhoon "Marie 1966" as revealed by Nimbus II high resolution infrared and ESSA-3 television data. NASA Technical Note. National Aeronautics and Space Administration, Washington, D. C. (In press).

LIST OF FIGURES

8. Tropical Disturbance "Marie 1966" as shown by Photo Imagery of Nimbus II High Resolution Infrared Radiometer (HRIR) data from orbits 2211, 2212, 2213 on 28 October 1966.

9. Tropical Disturbance "Marie 1966" analyzed from a grid print map of Nimbus II High Resolution Infrared Radiometer (HRIR) data from orbits 2212, 2213 on 28 October 1966 (1 grid interval = 0.625 degrees longitude).

10. Tropical Depression "Marie 1966" analyzed from a grid print map of Nimbus II High Resolution Infrared Radiometer (HRIR) data from orbits 2225, 2226 on 29 October 1966 (1 grid interval = 0.625 degrees longitude).

11. Typhoon "Marie 1966" analyzed from a grid print map of Nimbus II High Resolution Infrared Radiometer (HRIR) data from orbits 2265, 2266, 2267 on 1 November 1966 (1 grid interval = 0.625 degrees longitude).

12 Monthly Mean Sea Surface Temperature of the Pacific Ocean for October (from U.S. Naval Oceanographic Office, 1968) and track of "Marie 1966" from 25 October through 4 November 1966.

13. 200 MB Streamline analysis of 26 October 1966, 1200 GMT using radiosonde observations and satellite cloud pictures.

1. An example of Photo Imagery of Nimbus II High Resolution Infrared Radiometer (HRIR) Data from Orbit 2266 on 1 November 1966 showing Typhoon "Marie 1966" in the center.

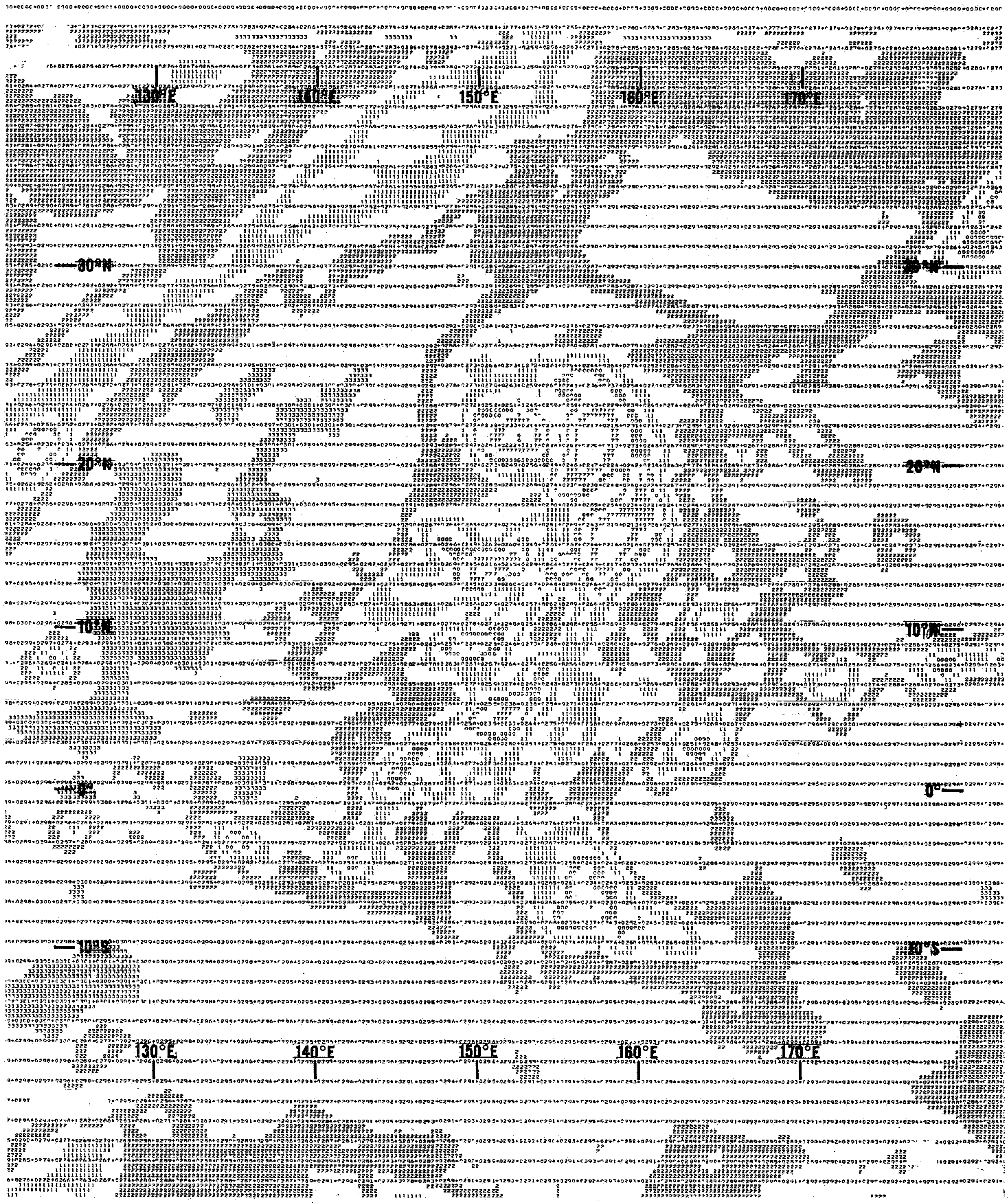

2. An example of a Composite Grid Print Map of Nimbus II High Resolution Infrared Radiometer (HRIR) Data from Orbits 2265, 2266, 2267 on 1 November 1966 Projected on a Mercator Base (1 grid interval = 1.25 degrees longitude), showing Typhoon "Marie 1966" in the center.

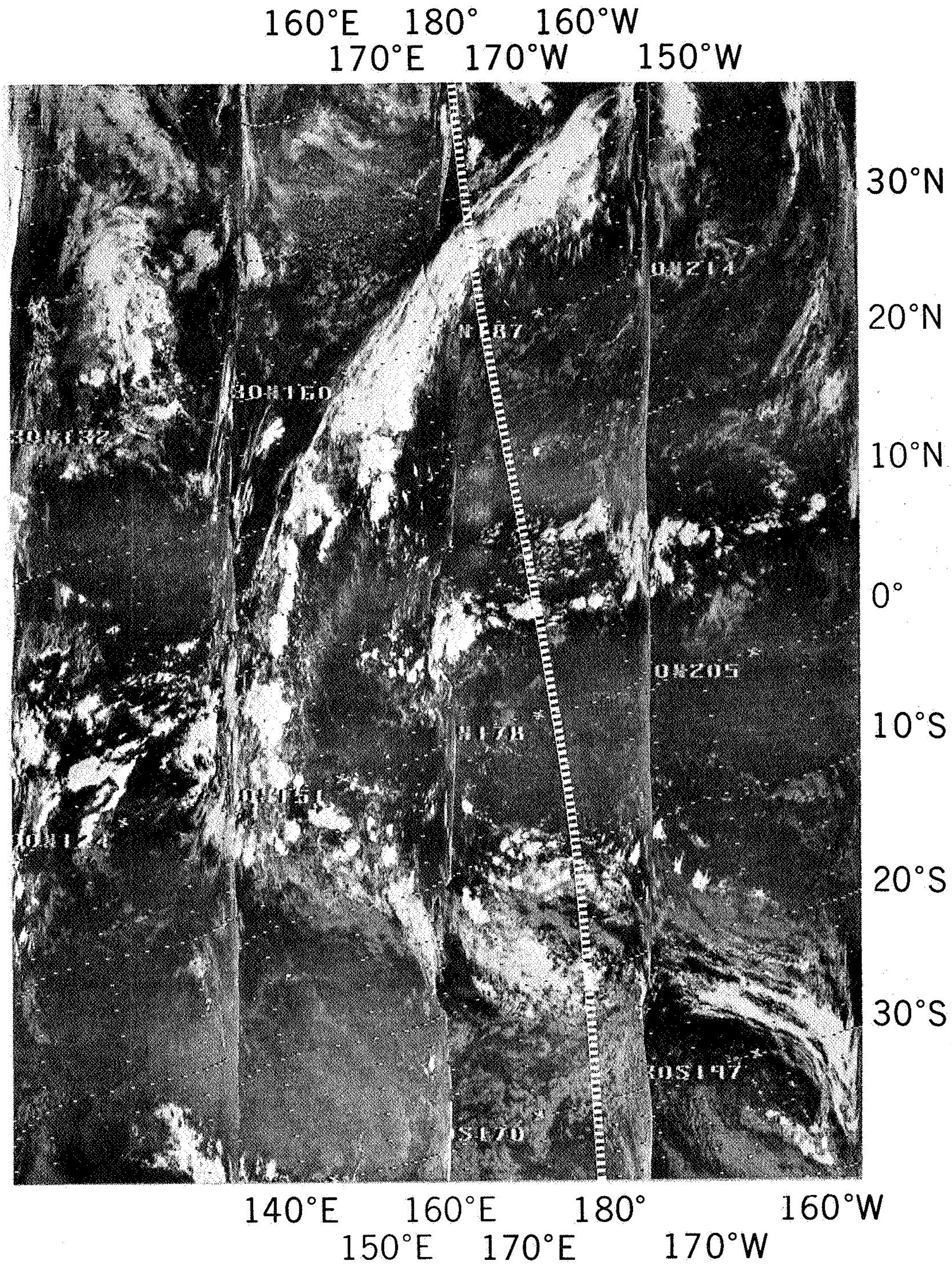

3. Formative Stage of "Marie 1966" as shown by Photo Imagery of Nimbus II High Resolution Infrared Radiometer (HRIR) data from orbits 2171, 2172, 2173, 2174 on 25 October 1966.

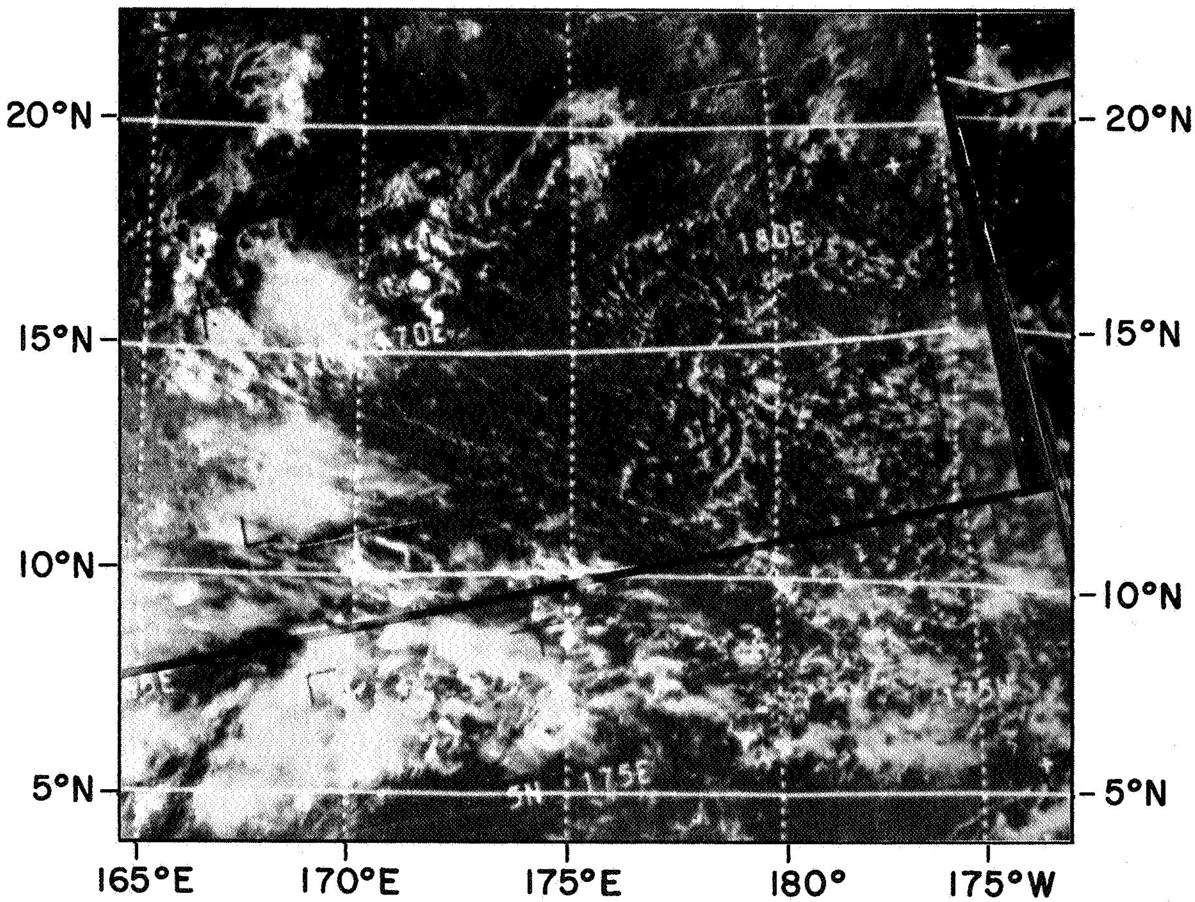

4. Formative Stage of "Marie 1966" as shown by ESSA III television pictures from orbit 284 on 25 October 1966.

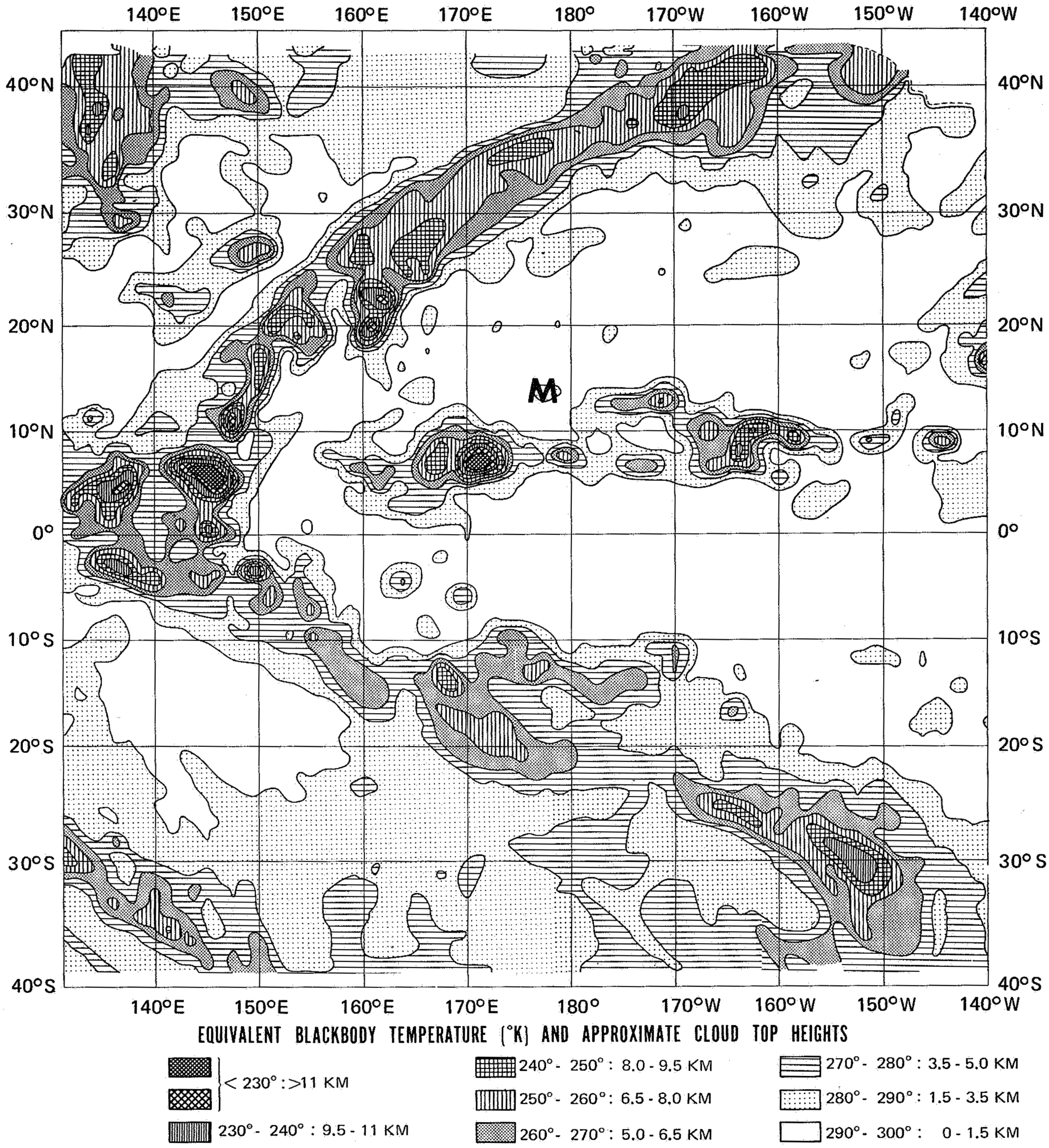

5. Formative Stage of "Marie 1966" analyzed from a grid print map of Nimbus II High Resolution Infrared Radiometer (HRIR) data from orbits 2171, 2172, 2173, 2174 on 25 October 1966 (1 grid interval = 1.25 degrees longitude).

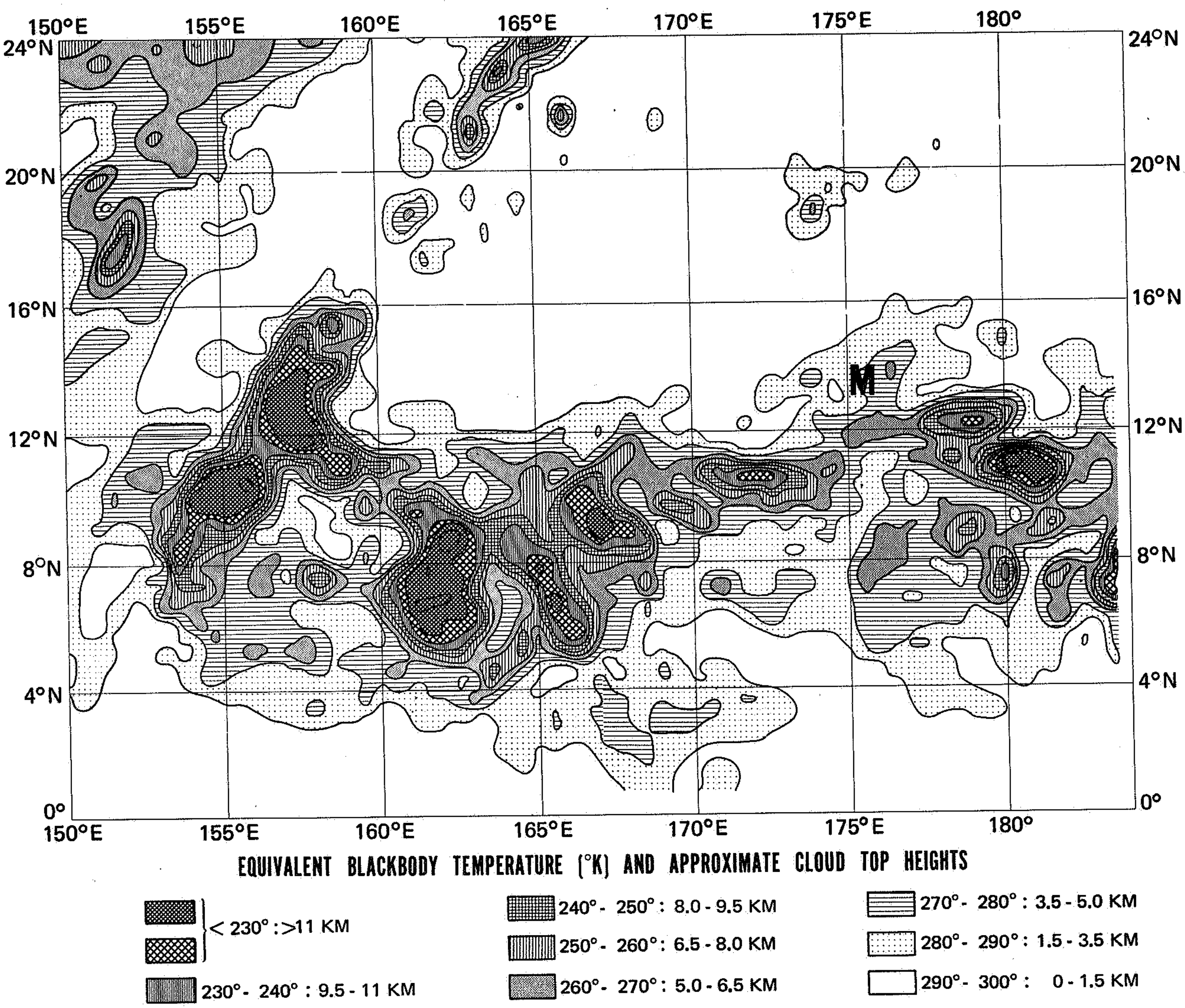

6. Formative Stage of "Marie 1966" analyzed from a grid print map of Nimbus II High Resolution Infrared Radiometer (HRIR) data from orbits 2185, 2186, 2187 on 26 October 1966 (1 grid interval = 0.625 degrees longitude).

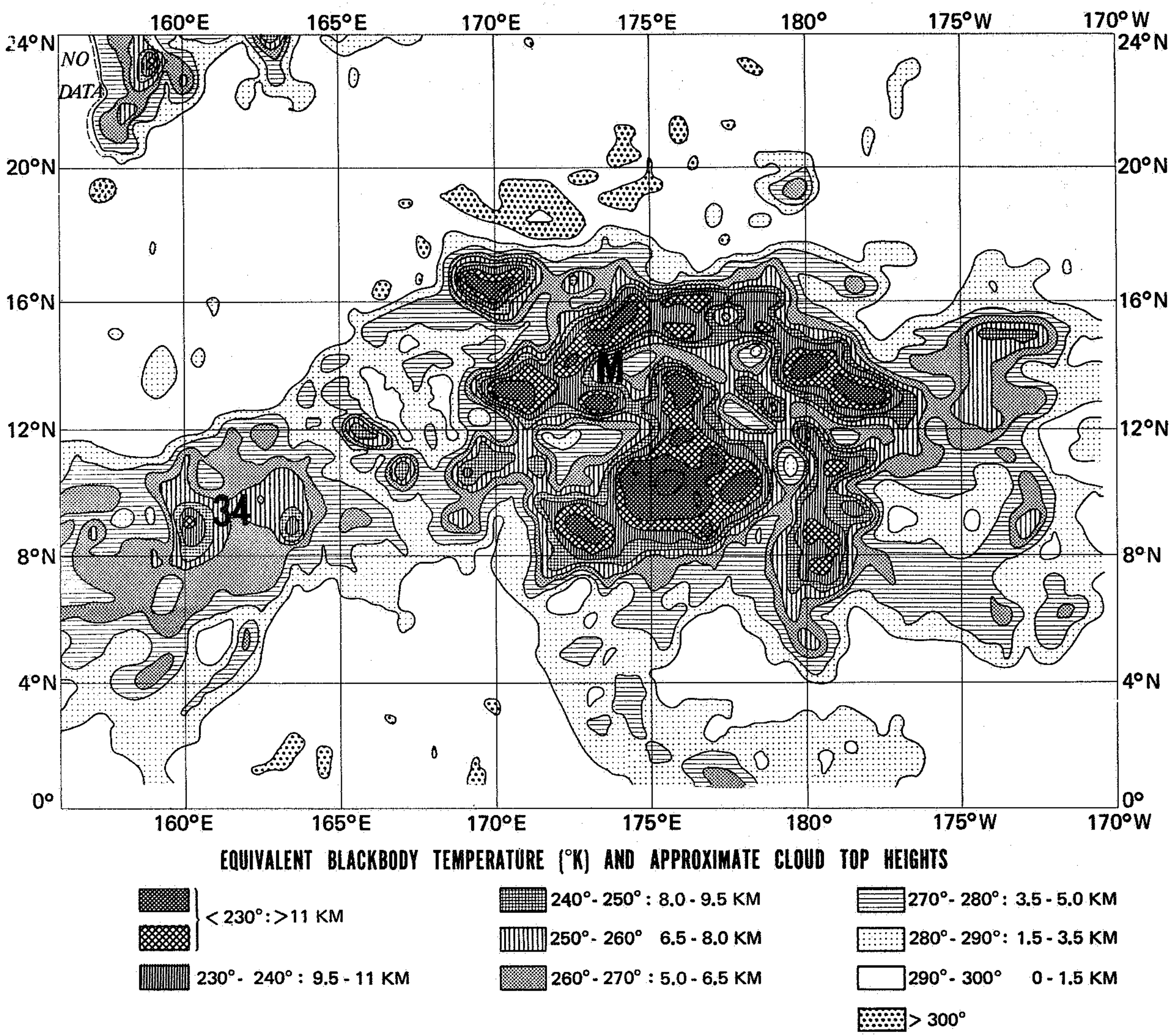

7. Tropical Disturbances "Marie 1966" analyzed from a grid print map of Nimbus II High Resolution Infrared Radiometer (HRIR) data from orbits 2198, 2199, 2200 on 27 October 1966 (1 grid interval = 0.625 degrees longitude).

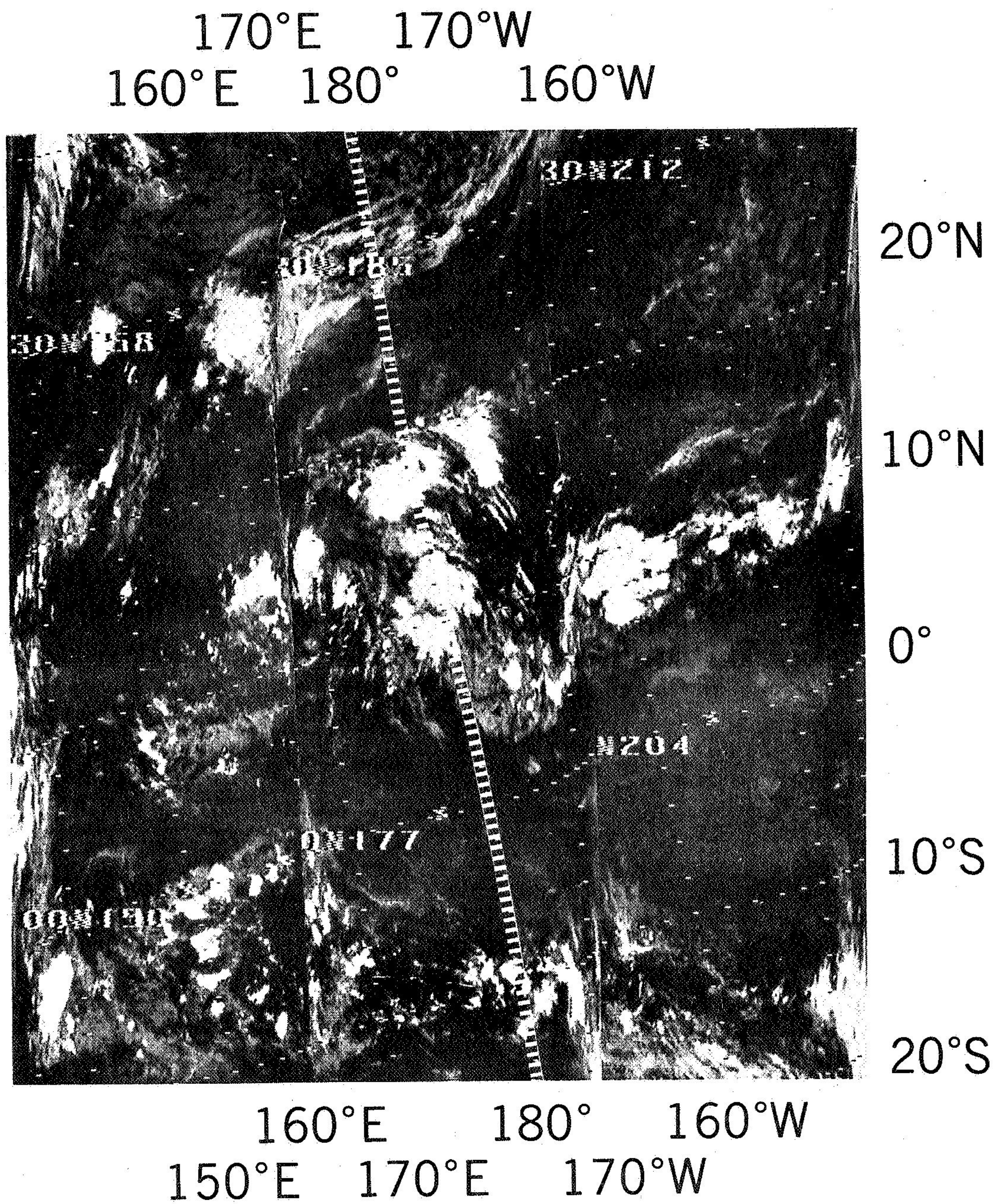

8. Tropical Disturbance "Marie 1966" as shown by Photo Imagery of Nimbus II High Resolution Infrared Radiometer (HRIR) data from orbits 2211, 2212, 2213 on 28 October 1966.

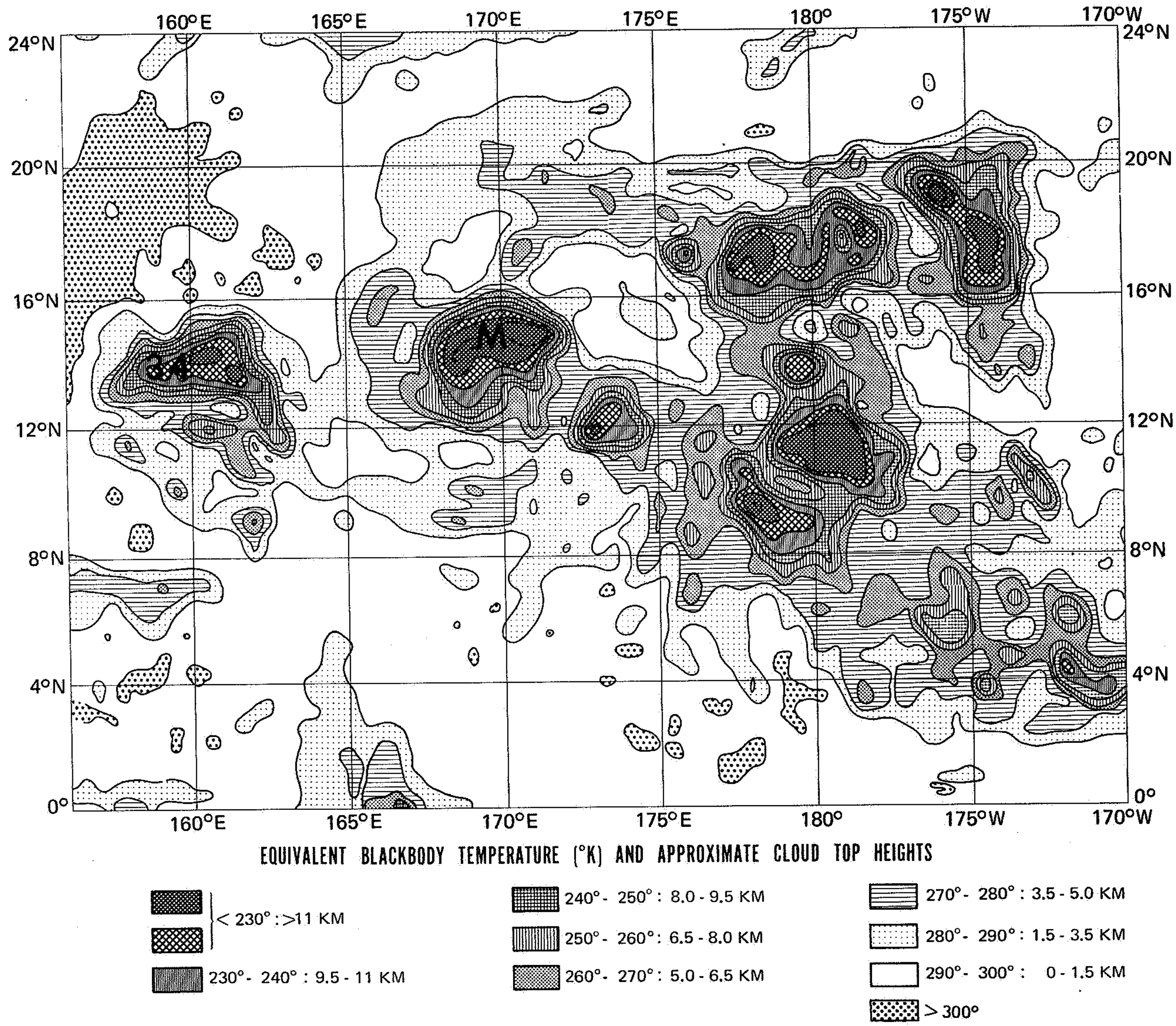

9. Tropical Disturbance "Marie 1966" analyzed from a grid print map of Nimbus II High Resolution Infrared Radiometer (HRIR) data from orbits 2212, 2213 on 28 October 1966 (1 grid interval = 0.625 degrees longitude).

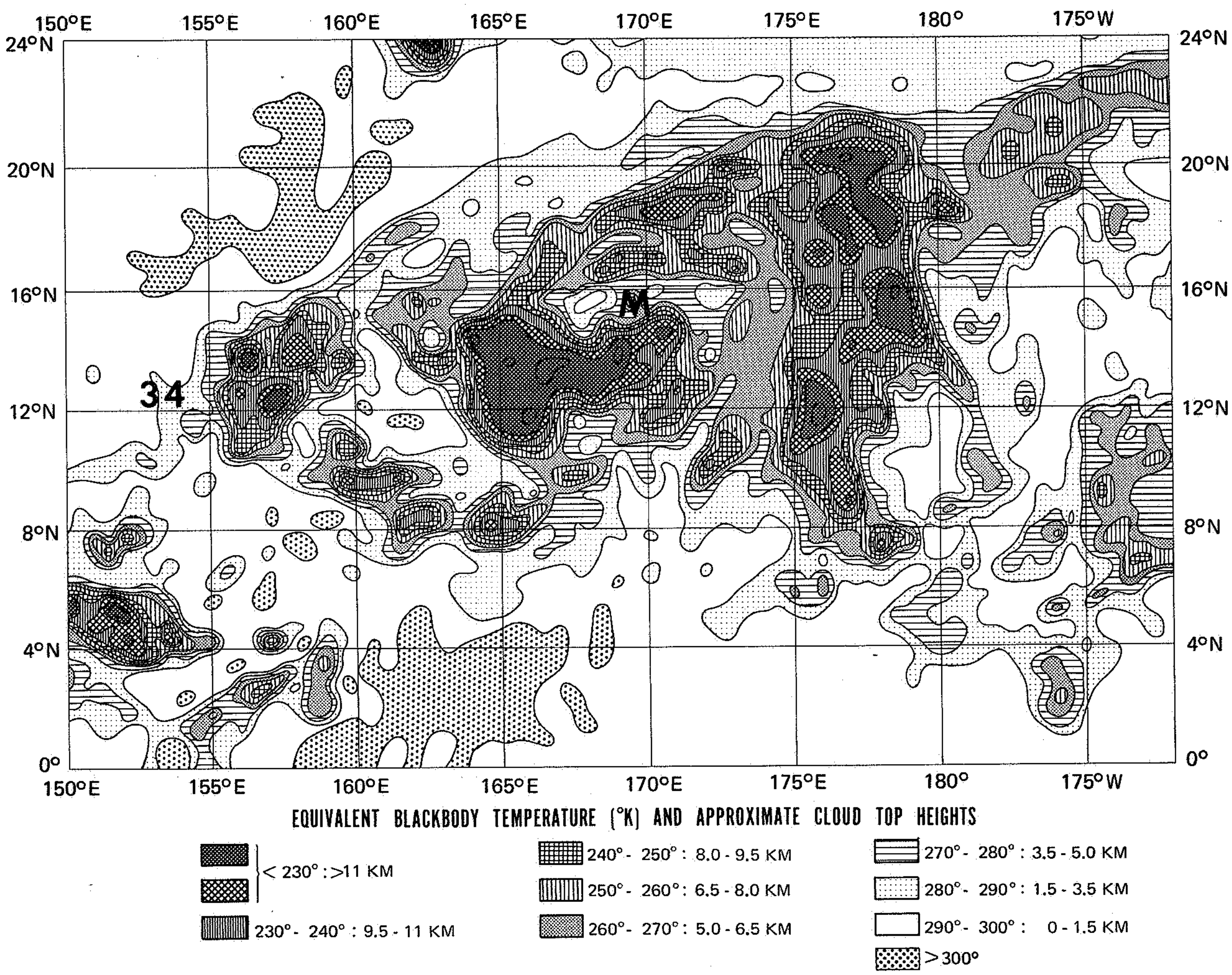

10. Tropical Depression "Marie 1966" analyzed from a grid print map of Nimbus II High Resolution Infrared Radiometer (HRIR) data from orbits 2225, 2226 on 29 October 1966 (1 grid interval = 0.625 degrees longitude).

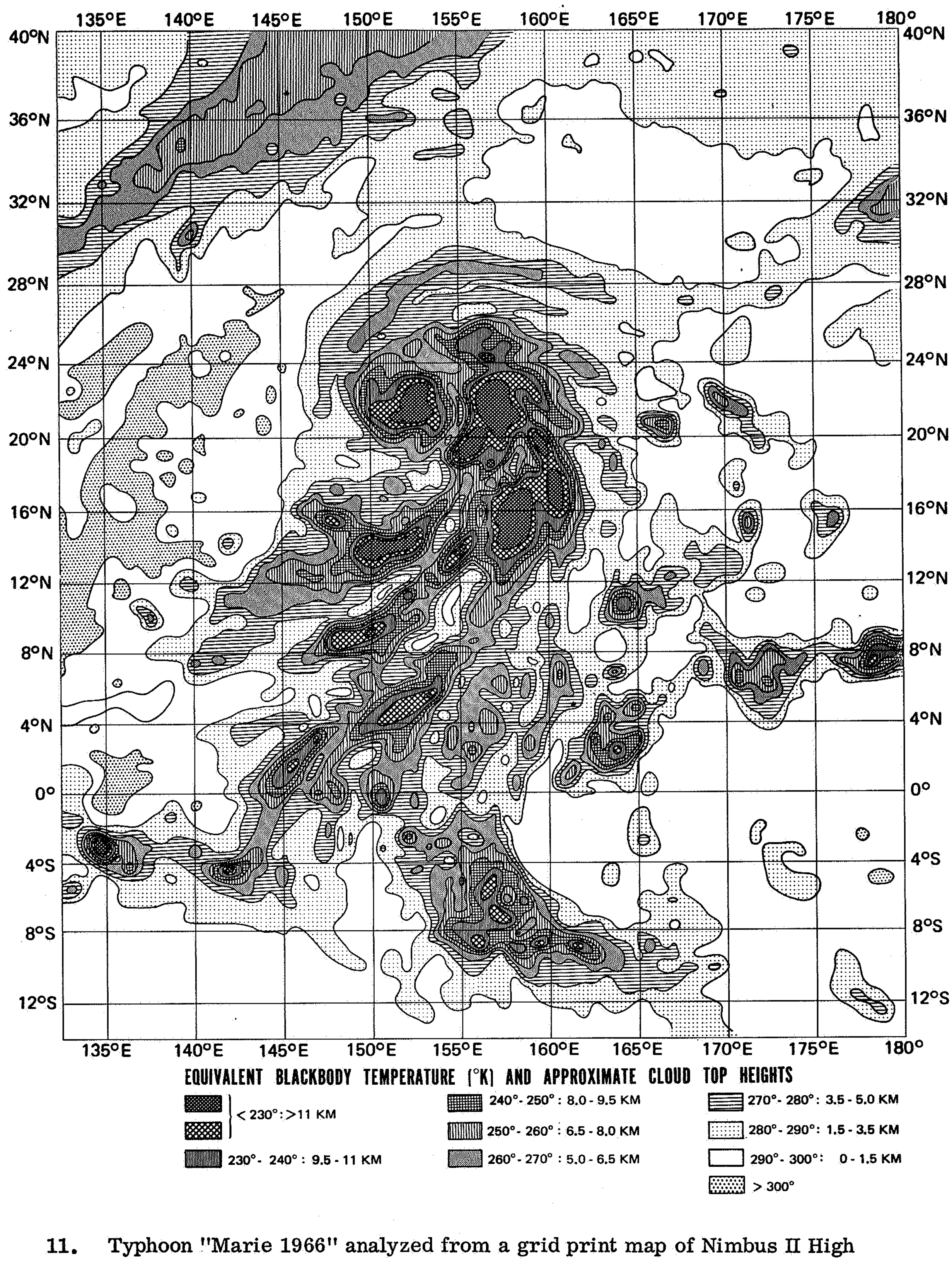

11. Typhoon "Marie 1966" analyzed from a grid print map of Nimbus II High Resolution Infrared Radiometer (HRIR) data from orbits 2265, 2266, 2267 on 1 November 1966 (1 grid interval = 0.625 degrees longitude).

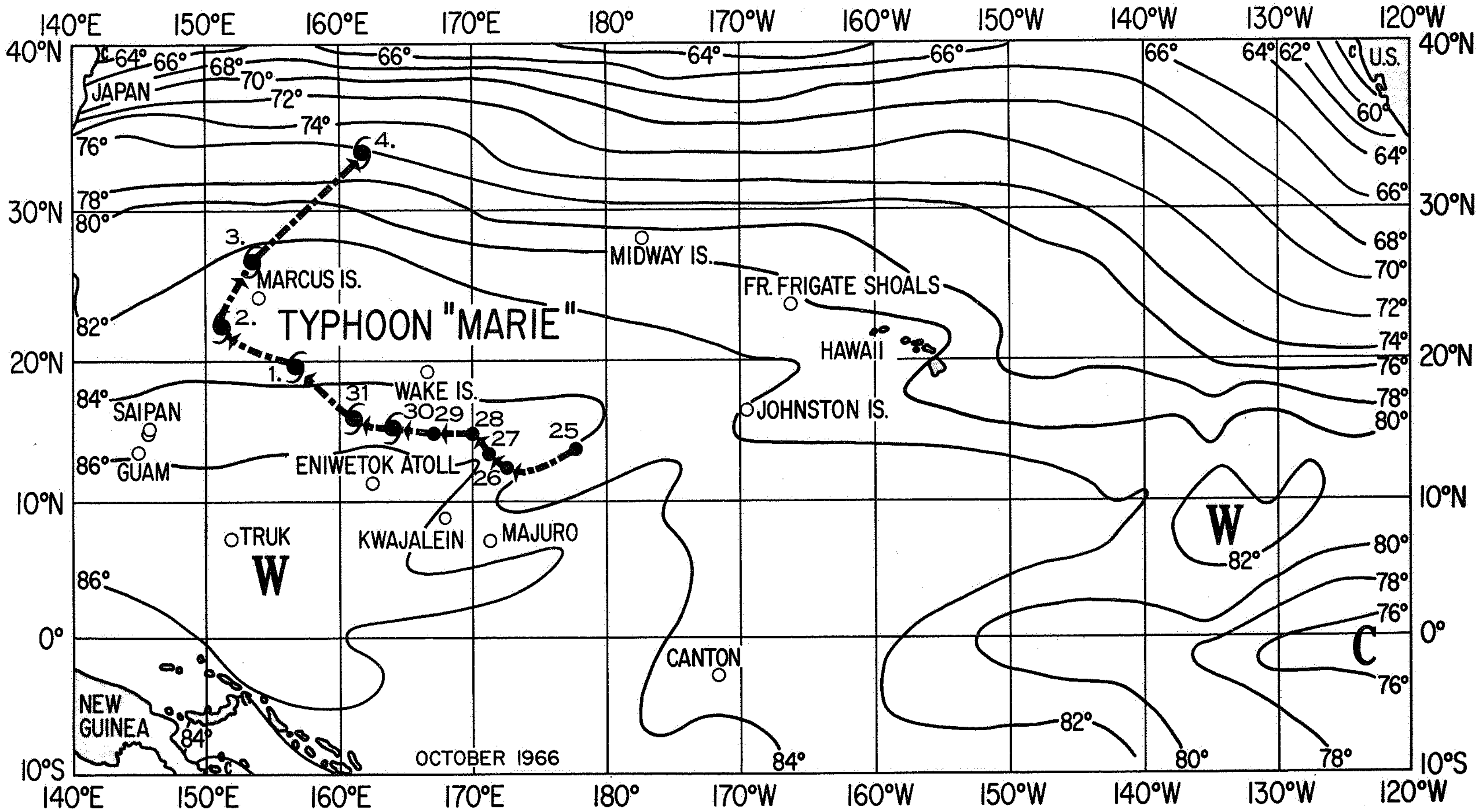

12 Monthly Mean Sea Surface Temperature of the Pacific Ocean for October (from U.S. Naval Oceanographic Office, 1968) and track of "Marie 1966" from 25 October through 4 November 1966.

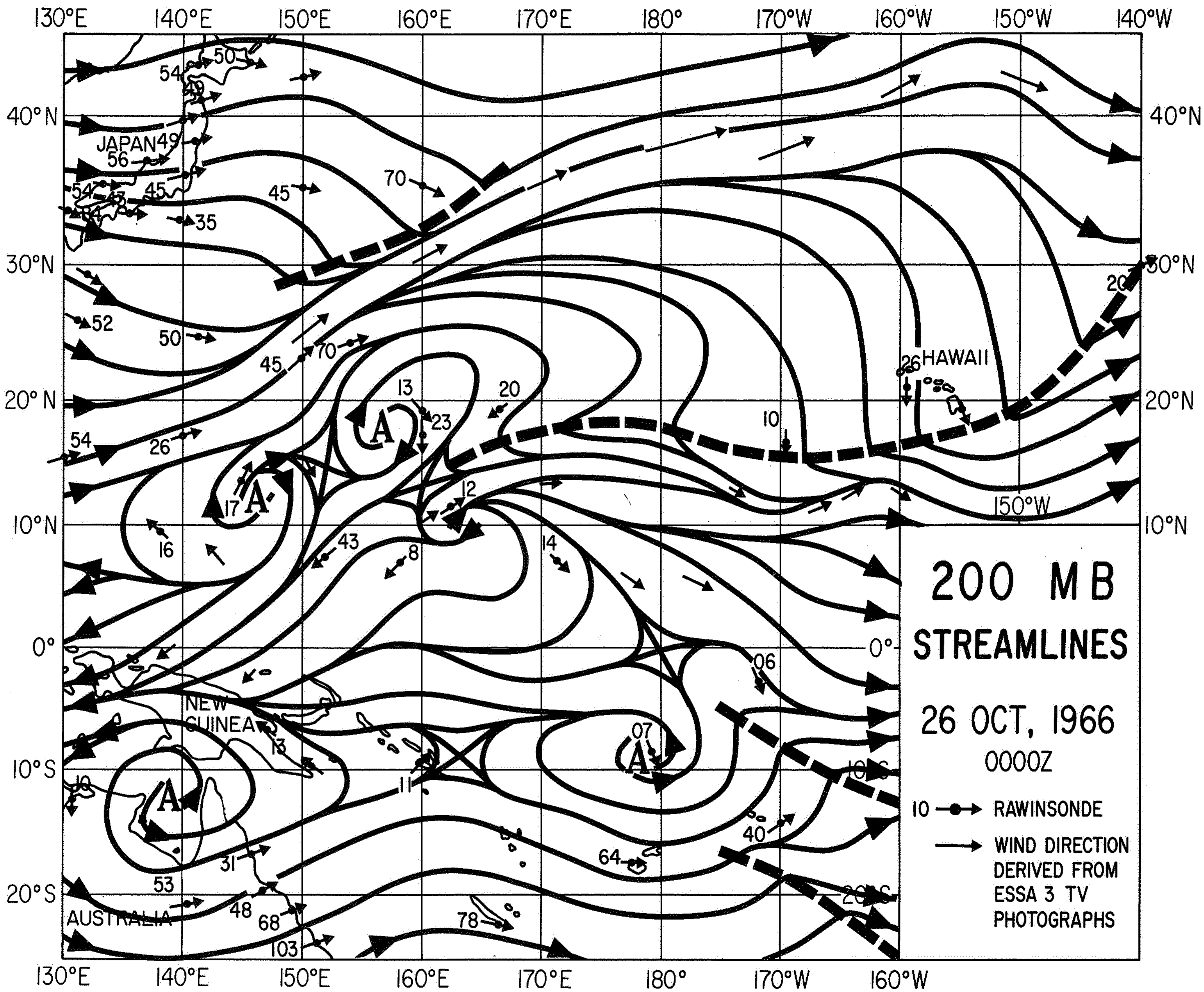

13. 200 MB Streamline analysis of 26 October 1966, 1200 GMT using radiosonde observations and satellite cloud pictures.